

Supplementary Information

This document presents supplementary figures showing the trend in precipitation.

Projection task

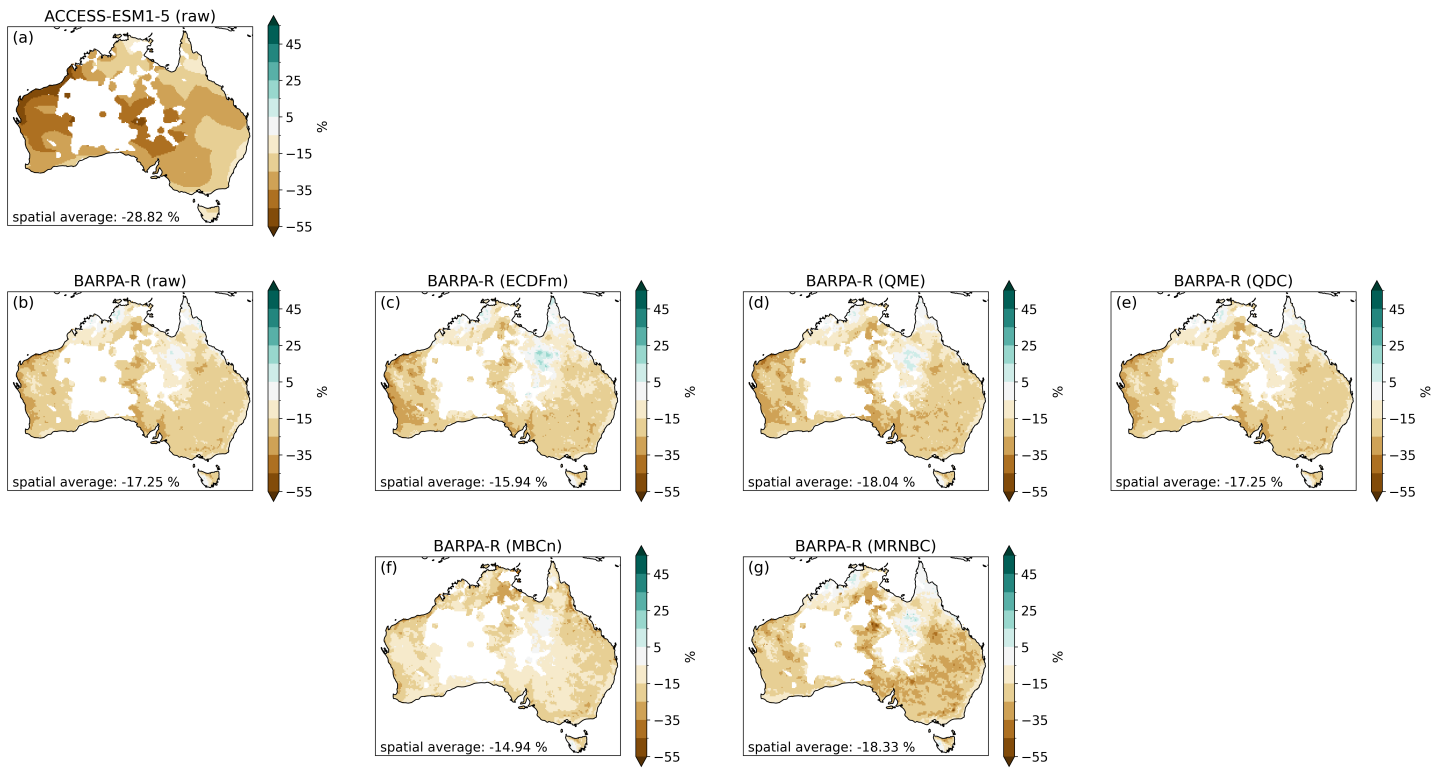


Figure S1: Change in annual mean precipitation between 1980-2019 and 2060-2099 for the projection assessment task. Results are shown for the ACCESS-ESM1-5 GCM (panel a), the BARPA-R RCM forced by that GCM (panel b), and for various bias correction methods applied to those RCM data (panels c-g). Land areas where the AGCD data are unreliable due to weather station sparsity have been masked in white.

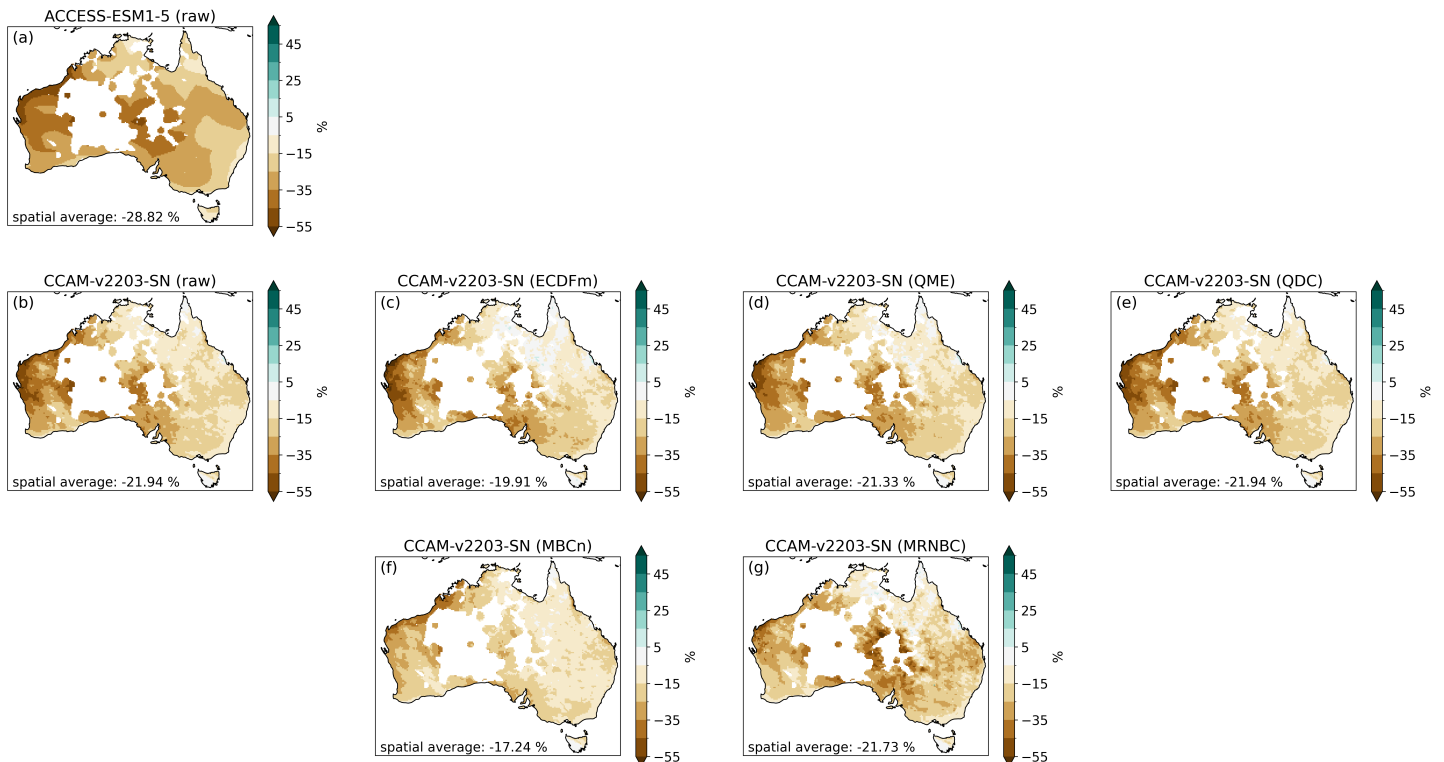


Figure S2: Change in annual mean precipitation between 1980-2019 and 2060-2099 for the projection assessment task. Results are shown for the ACCESS-ESM1-5 GCM (panel a), the CCAM-v2203-SN RCM forced by that GCM (panel b), and for various bias correction methods applied to those RCM data (panels c-g). Land areas where the AGCD data are unreliable due to weather station sparsity have been masked in white.

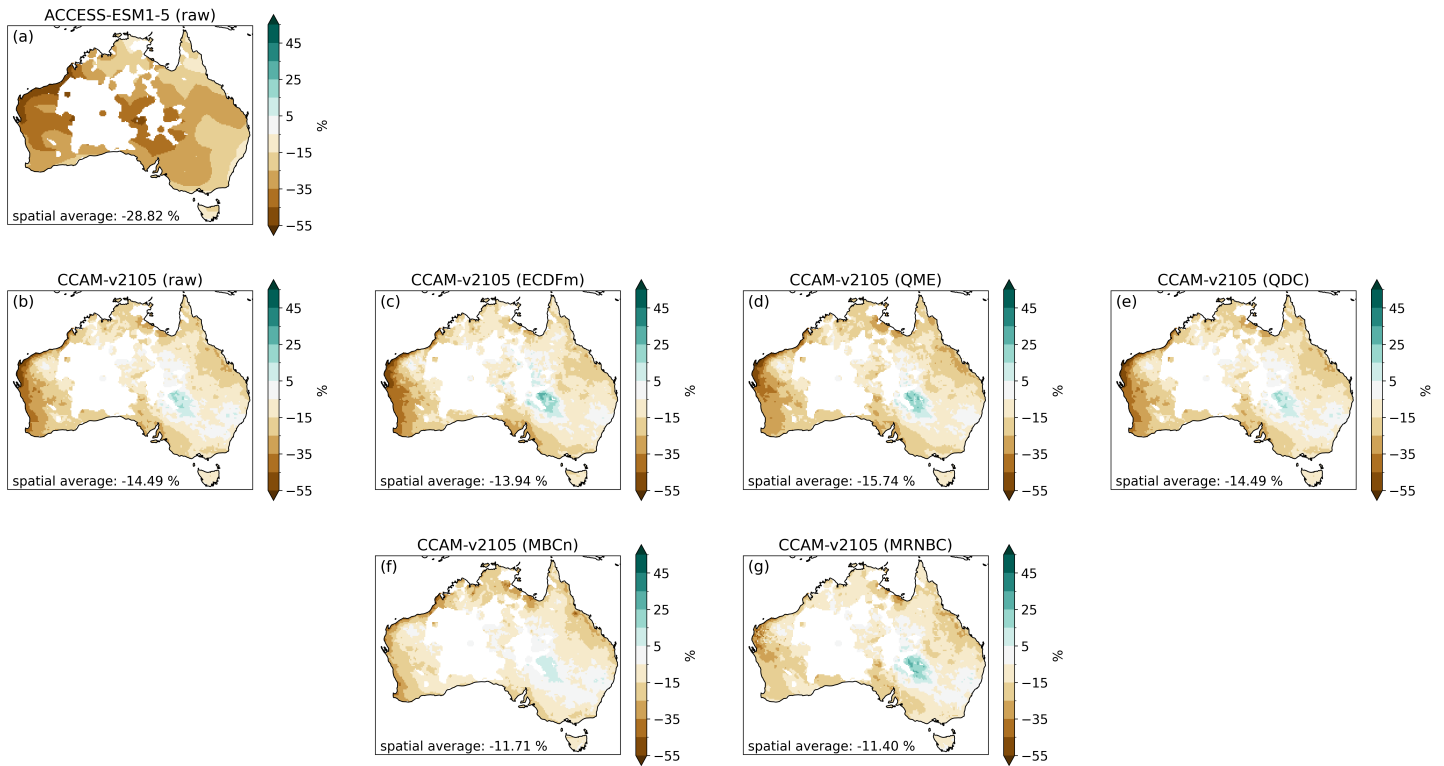


Figure S3: Change in annual mean precipitation between 1980-2019 and 2060-2099 for the projection assessment task. Results are shown for the ACCESS-ESM1-5 GCM (panel a), the CCAM-v2105 RCM forced by that GCM (panel b), and for various bias correction methods applied to those RCM data (panels c-g). Land areas where the AGCD data are unreliable due to weather station sparsity have been masked in white.

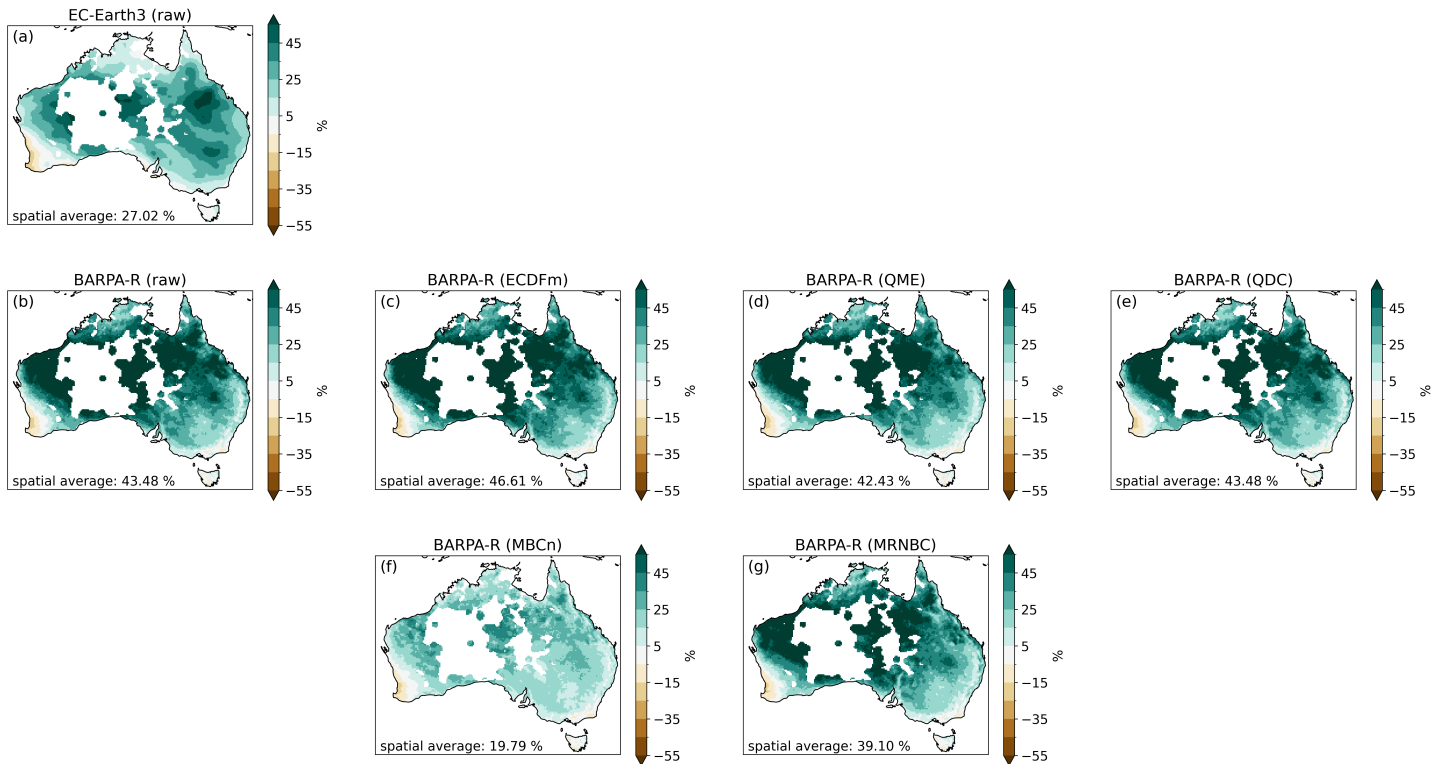


Figure S4: Change in annual mean precipitation between 1980-2019 and 2060-2099 for the projection assessment task. Results are shown for the EC-Earth3 GCM (panel a), the BARPA-R RCM forced by that GCM (panel b), and for various bias correction methods applied to those RCM data (panels c-g). Land areas where the AGCD data are unreliable due to weather station sparsity have been masked in white.

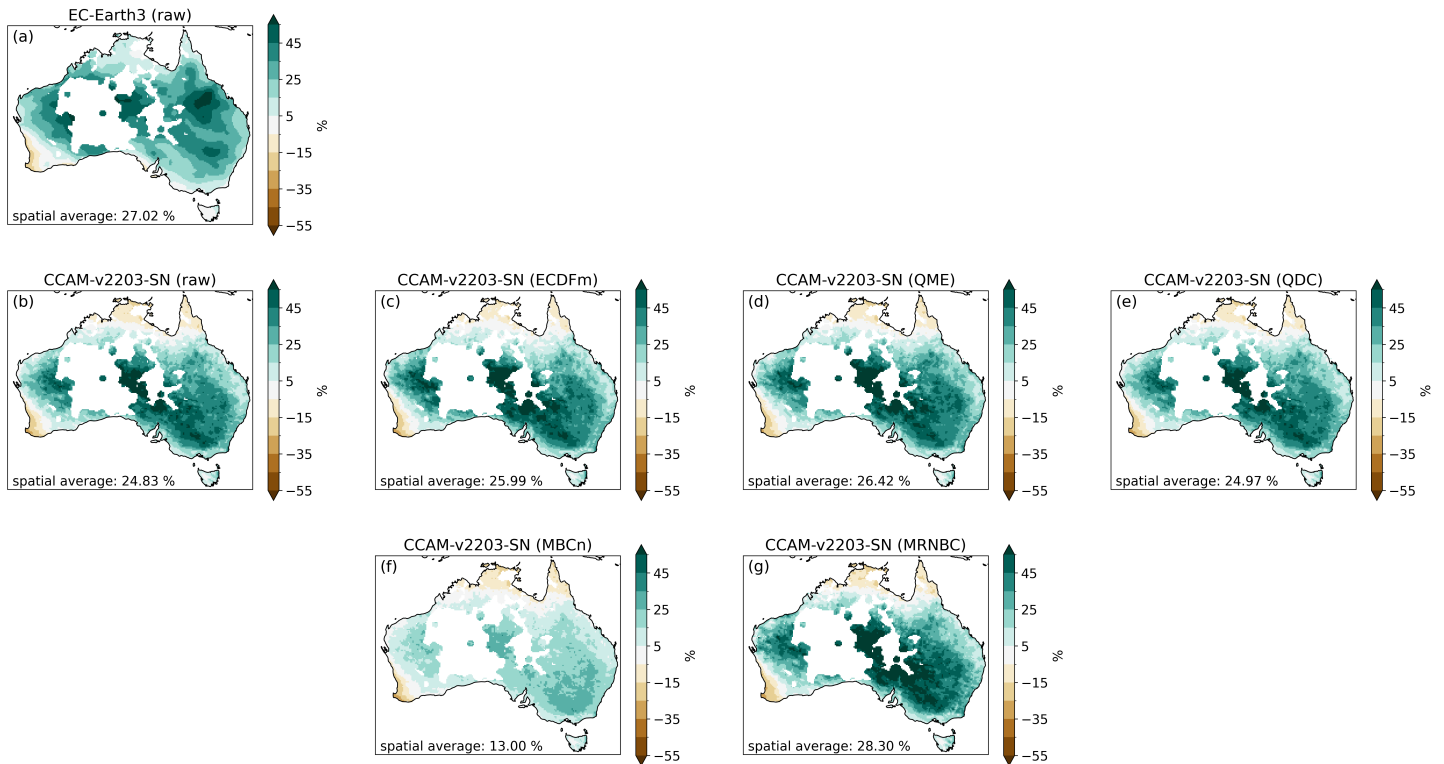


Figure S5: Change in annual mean precipitation between 1980-2019 and 2060-2099 for the projection assessment task. Results are shown for the EC-Earth3 GCM (panel a), the CCAM-v2203-SN RCM forced by that GCM (panel b), and for various bias correction methods applied to those RCM data (panels c-g). Land areas where the AGCD data are unreliable due to weather station sparsity have been masked in white.

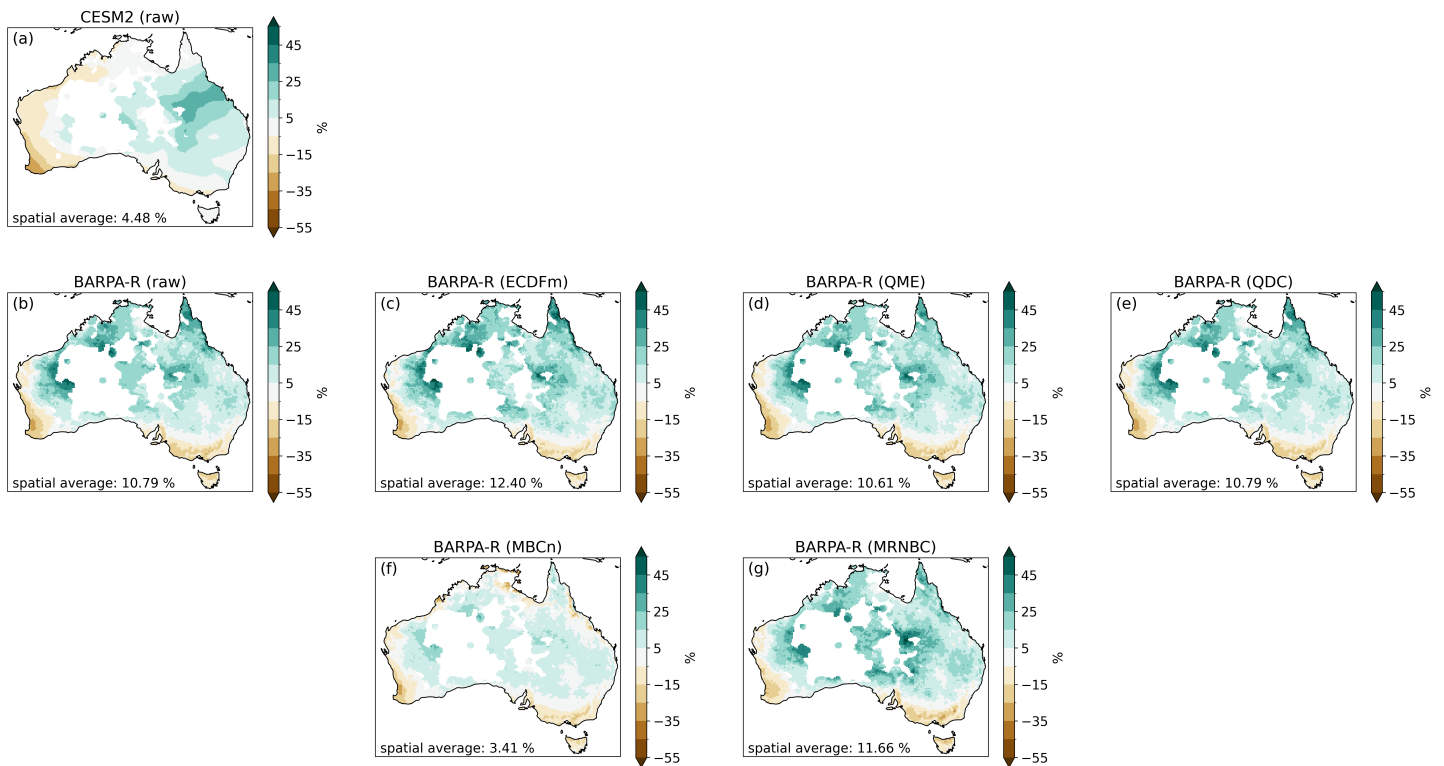


Figure S6: Change in annual mean precipitation between 1980-2019 and 2060-2099 for the projection assessment task. Results are shown for the CESM2 GCM (panel a), the BARPA-R RCM forced by that GCM (panel b), and for various bias correction methods applied to those RCM data (panels c-g). Land areas where the AGCD data are unreliable due to weather station sparsity have been masked in white.

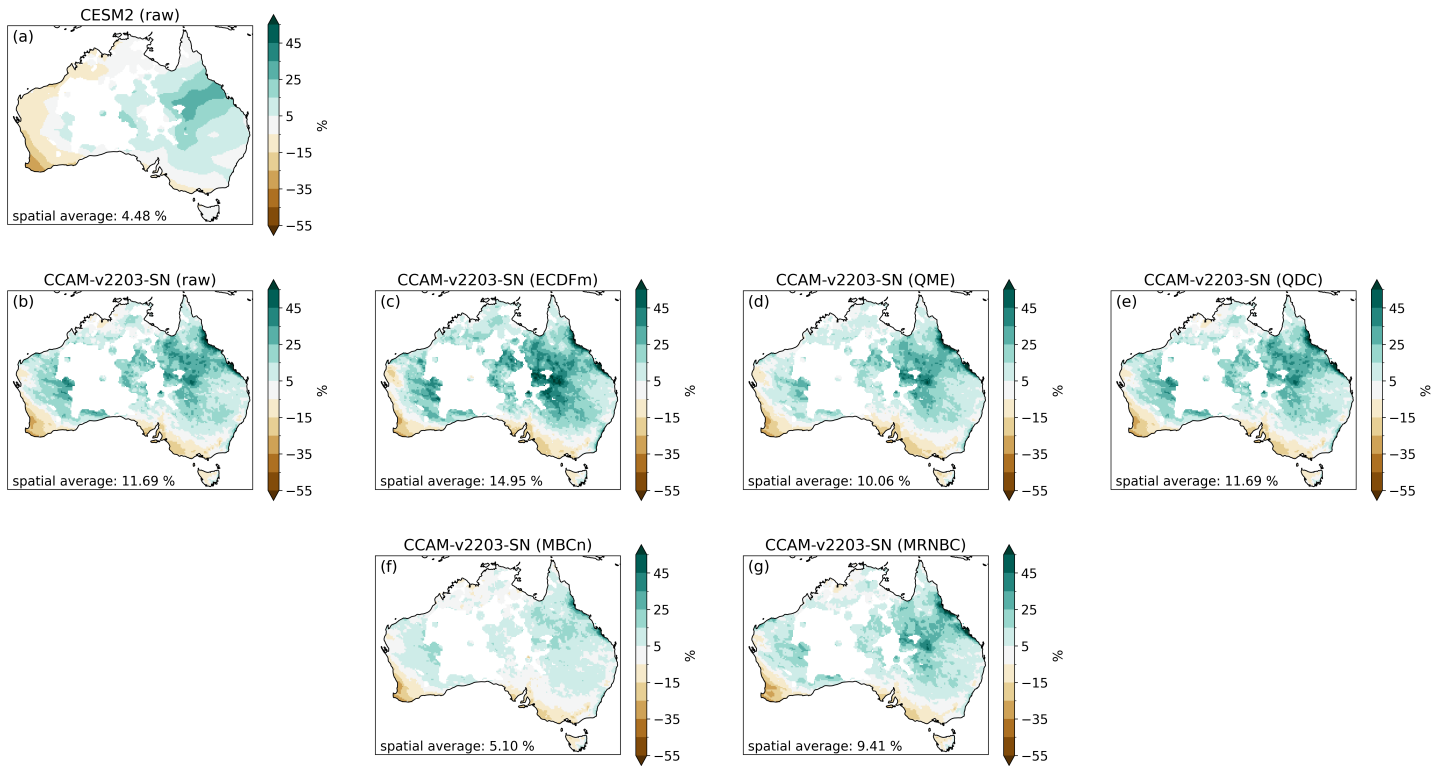


Figure S7: Change in annual mean precipitation between 1980-2019 and 2060-2099 for the projection assessment task. Results are shown for the CESM2 GCM (panel a), the CCAM-v2203-SN RCM forced by that GCM (panel b), and for various bias correction methods applied to those RCM data (panels c-g). Land areas where the AGCD data are unreliable due to weather station sparsity have been masked in white.